

Contents

Page

Launch of the new JMA's One-month Guidance Tool	1
Incorporation of Standardized Precipitation Index (SPI) for drought monitoring into the ClimatView tool	2
El Niño Outlook (June – December 2019)	3
JMA's Seasonal Numerical Ensemble Prediction for Boreal Summer 2019	5
Warm Season Outlook for Summer 2019 in Japan	7
Summary of the 2018/2019 Asian Winter Monsoon	8
TCC contributions to Regional Climate Outlook Forums in Asia	14
JMA Advisory Panel on Extreme Climate Events: collaboration between research and operation in Japan to provide useful climate services	15

Launch of the new JMA's One-month Guidance Tool

TCC has launched a new interactive tool enabling the generation of statistical guidance for station points in support of operational seasonal forecasts covering periods of a month or less. This handy resource is in the form of a web-based application accessed via a browser on the TCC website at:

- <https://ds.data.jma.go.jp/tcc/tcc/products/model/index.html> (see the bottom of the "One-month Prediction" section)
- https://extreme.kishou.go.jp/cgi-bin/simple_guidance/index.cgi (for the password required, see the bottom of this article).

The user simply provides past observation data to create guidance forecasting. Past and real-time forecast data from JMA's ensemble prediction system are stored on the application side. The following figures and data for the selected forecast period are automatically created and displayed on the screen (Figure 1) after interactive parameter settings (initial day, forecast periods and predictor elements (Figure 2)) and background calculation:

- Tercile probability map
- Figure(s) on tercile probability (color bars) at station(s)
- Inter-annual time-series representation of tercile probability
- Diagram showing reliability and forecast frequency
- The CSV-format data file used to create the above

For more details and system specifications, see the online help page at:

https://extreme.kishou.go.jp/tool/simple_guidance/help/ (tool commentary).

Forecast datasets are updated every Thursday.

As the tool provides forecasts and related materials, access is exclusive to National Meteorological and Hydrological Service (NMHS) staff. To gain access, email TCC (tcc@met.kishou.go.jp) stating your 1) name, 2) affiliation, 3) email address and 4) purpose of use. The tool is currently operated on an experimental basis and, despite TCC's dedication to its development, may be changed or service may be suspended without notice in the event of malfunction or other issues. Your understanding in this regard is appreciated.

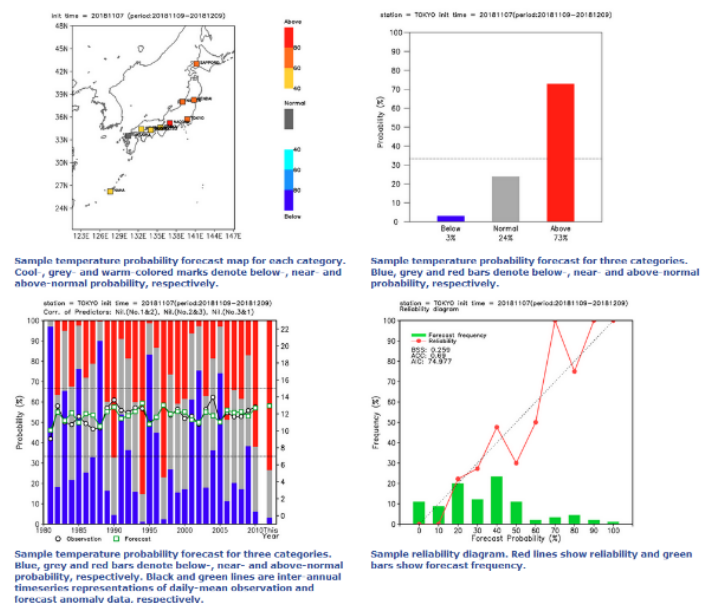


Figure 1 Examples of simple guidance tool output

We expect that this tool is useful for issuing seasonal forecast for one-month or less in terms of simply generating statistical guidance. TCC welcomes your comments/suggestions so that the tool will be further improved for use at respective NMHSs.

(Yasushi Mochizuki, Tokyo Climate Center)

JMA's One-month Guidance Tool (Commentary)

Initial date: 20190515 → The beginning and ending date of the valid time will be automatically set on the next pull-down menu.
 Forecast period: 2019 / 5 / 17 → 2019 / 6 / 16
 Predictor: Surface temperature / 850-hPa meridional wind -- No.3 --
 Station and observation data: (Sample text data: Temperature, Precipitation)
 Choose File: no file selected

```
#elname=temperature,,,,,,,,,,,,,
#lonlat=9999,,,,,,,,,,,,,
#station=,, , TOKYO, MIYATA, SENDAI, NAGOYA, OSAKA, SAPPORO, HIROSHIMA, TAKAMATSU, FUKUOKA, NAHA
#lon=,, , 139.75, 139.140, 137.135, 135.5, 141.2, 132.5, 134, 130.4, 127.6
#lat=,, , 35.691, 36.38, 35.35, 34.6, 43, 34.4, 34.3, 33.5, 26.2
1981, 1, 1, 5, 2, 2, 1, 0, 3, 4, 4, 6, -3, 3, 2, 7, 2, 8, 5, 3, 15, 6
1981, 1, 2, 4, 6, 4, 3, 2, 9, 3, 5, 5, -2, 2, 2, 9, 4, 6, 2, 7, 13, 4
1981, 1, 3, 5, 1, 4, 3, 1, 1, 2, 2, 3, -0, 3, 1, 2, 2, 8, 2, 2, 13, 3
1981, 1, 4, 4, 4, 4, 7, 1, 9, 1, 7, 2, 9, -2, 4, 1, 5, 2, 8, 2, 1, 14, 2
1981, 1, 5, 4, 1, 3, 2, 9, 0, 1, 8, 2, 7, -6, 7, 2, 2, 7, 3, 4, 14, 9
1981, 1, 6, 3, 5, 2, -0, 7, 1, 3, 2, 7, -6, 1, 9, 2, 9, 2, 9, 15, 3
```

 Detailed Options | Submit

Figure 2 Parameter setting section

[Table of contents](#)

Incorporation of Standardized Precipitation Index (SPI) for drought monitoring into the ClimatView tool

TCC began providing worldwide drought monitoring information via its interactive online ClimatView tool in March 2019 to assist National Meteorological and Hydrological Services (NMHSs) in their monitoring of current and historical drought statuses.

For this resource, TCC uses Standardized Precipitation Index (SPI) data as a measure of the degree of prolonged rainfall deficit. The tool displays SPI values for periods of 3, 6 and 12 months to help users quantify precipitation deficits on multiple timescales. This detailed drought information can be accessed on the TCC website at <https://ds.data.jma.go.jp/tcc/tcc/products/climate/climatview/frame.php> (main page) https://ds.data.jma.go.jp/tcc/tcc/products/climate/climatview/spi_commentary.html (SPI commentary)

The tool shows SPI values covering the period from June 1982 to the present in the following formats:

- Geographical distribution maps (global and regional, Figure 3)

- Time-series graphs (Figure 4) with corresponding data tables and downloadable CSV files
- Regional listings
- Printable figures

Calculation of the SPI values shown in the tool is based on monthly precipitation totals from CLIMAT data for states worldwide and on Global Historical Climatology Network (GHCN) data provided by the National Oceanic and Atmospheric Administration (NOAA)'s National Centers for Environmental Information. TCC uses the SPI calculation program provided by Colorado State University in the USA. See the commentary webpage for an outline of the SPI and more details on data and methods.

We expect that this handy tool is useful for monitoring current and historical drought conditions. TCC welcomes your comments/suggestions so that the tool will be further improved for use at respective NMHSs.

(Yasushi Mochizuki, Tokyo Climate Center)

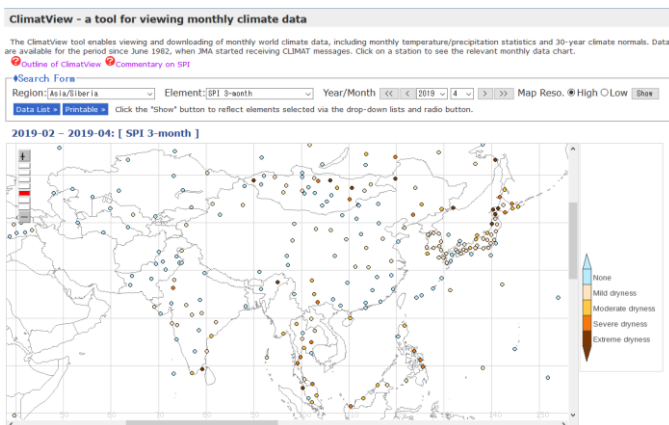


Figure 3 Geographical distribution map (global)
 Note) SPI values are not calculated if the available historical data span is shorter than 30 years.

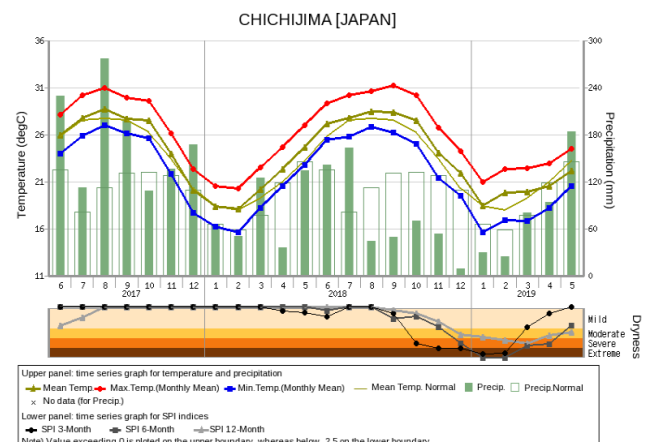


Figure 4 Time-series graph

[Table of contents](#)

El Niño Outlook (June – December 2019)

The El Niño conditions observed in the equatorial Pacific since boreal autumn 2018 are likely (70%) to continue until boreal summer. The likelihood of El Niño conditions continuing until boreal autumn (60%) is higher than that of ENSO-neutral conditions returning (40%). (Article based on the El Niño outlook issued on 10 June 2019.)

El Niño/La Niña

The NINO.3 SST deviation was $+0.6^{\circ}\text{C}$ in May. SSTs were above normal in most of the equatorial Pacific except the area around Indonesia (Figures 5 and 7 (a)), and subsurface temperatures were above normal mainly in the central part (Figures 6 and 7 (b)). Atmospheric convective activity near the date line over the equatorial Pacific was above normal, and easterly winds in the lower troposphere (trade winds) over the central equatorial Pacific were weaker than normal. Based on these factors, the El Niño conditions observed in the equatorial Pacific since boreal autumn 2018 are considered to remain ongoing.

The subsurface warm waters, which were observed mainly in the central equatorial Pacific, are expected to migrate eastward and to maintain warmer-than-normal SST conditions in the eastern part. JMA's El Niño prediction model suggests that the NINO.3 SST will be above or near normal from boreal summer to autumn, while uncertainties in model prediction are large (Figure 8). Based on this prediction and the observations described above, there is considered to be a 70% probability that the five-month running mean NINO.3 SST in early boreal summer will be $+0.5^{\circ}\text{C}$ or above and a 60% probability that this value in early boreal autumn will be $+0.5^{\circ}\text{C}$ or above (Figure 9). In conclusion, the El Niño conditions are likely (70%) to continue until boreal summer. The likelihood of El Niño conditions continuing until boreal autumn (60%) is higher than that of ENSO-neutral conditions returning (40%).

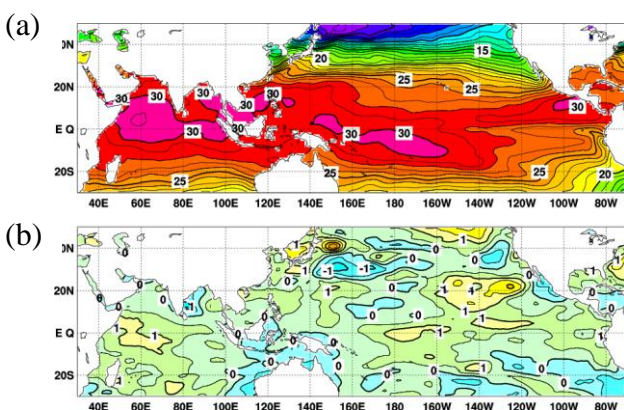


Figure 5 Monthly mean (a) sea surface temperatures (SSTs) and (b) SST anomalies in the Indian and Pacific Ocean areas for May 2019

The contour intervals are 1°C in (a) and 0.5°C in (b). The base period for the normal is 1981 – 2010.

Western Pacific and Indian Ocean

The area-averaged SST in the tropical western Pacific (NINO.WEST) region was near normal in May. The value is likely to be near normal from boreal summer to autumn.

The area-averaged SST in the tropical Indian Ocean (IOBW) region was above normal in May. The value is likely to be above or near normal from boreal summer to autumn.

(Hiroyuki Sugimoto, Tokyo Climate Center)

* The SST normal for the NINO.3 region ($5^{\circ}\text{S} - 5^{\circ}\text{N}$, $150^{\circ}\text{W} - 90^{\circ}\text{W}$) is defined as a monthly average over the latest sliding 30-year period (1989-2018 for this year).

* The SST normals for the NINO.WEST region ($\text{Eq.} - 15^{\circ}\text{N}$, $130^{\circ}\text{E} - 150^{\circ}\text{E}$) and the IOBW region ($20^{\circ}\text{S} - 20^{\circ}\text{N}$, $40^{\circ}\text{E} - 100^{\circ}\text{E}$) are defined as linear extrapolations with respect to the latest sliding 30-year period, in order to remove the effects of significant long-term warming trends observed in these regions.

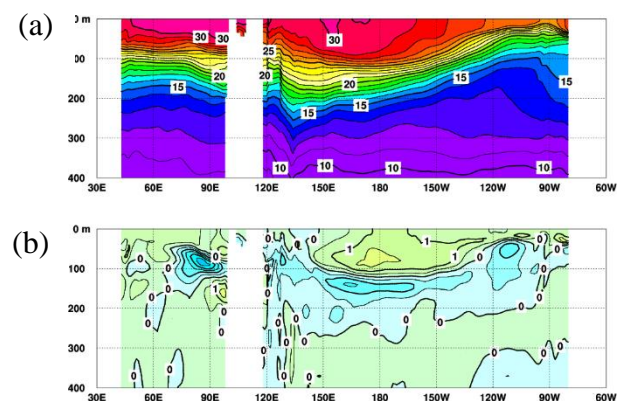


Figure 6 Monthly mean depth-longitude cross sections of (a) temperatures and (b) temperature anomalies in the equatorial Indian and Pacific Ocean areas for May 2019

The contour intervals are 1°C in (a) and 0.5°C in (b). The base period for the normal is 1981 – 2010.

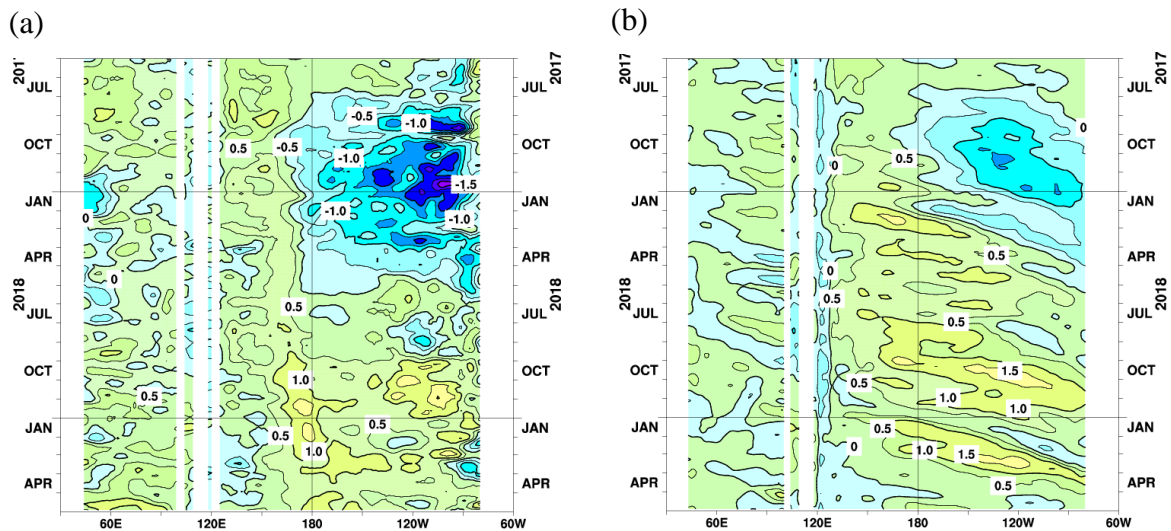


Figure 7 Time-longitude cross sections of (a) SST and (b) ocean heat content (OHC) anomalies along the equator in the Indian and Pacific Ocean areas
 OHCs are defined here as vertical averaged temperatures in the top 300 m. The base period for the normal is 1981 – 2010.

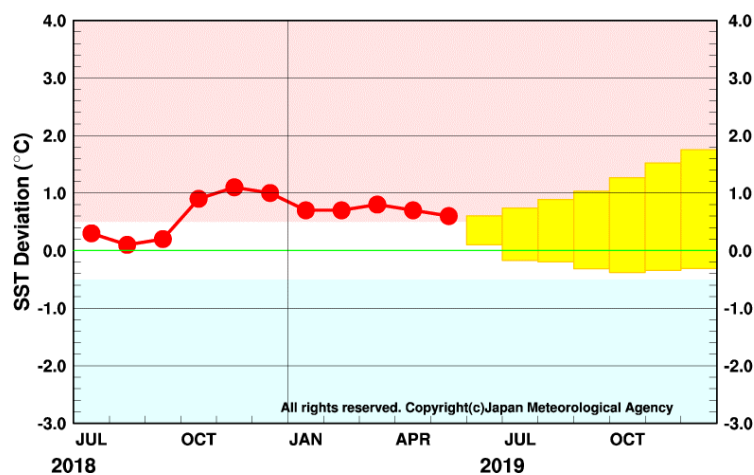


Figure 8 Outlook of NINO.3 SST deviation produced by the El Niño prediction model

This figure shows a time series of monthly NINO.3 SST deviations. The thick line with closed circles shows observed SST deviations, and the boxes show the values produced for up to six months ahead by the El Niño prediction model. Each box denotes the range into which the SST deviation is expected to fall with a probability of 70%.

YEAR	MONTH	mean period	El Niño	ENSO neutral	La Niña
2019	APR	FEB2019–JUN2019	100		
	MAY	MAR2019–JUL2019	100		
	JUN	APR2019–AUG2019	70	30	
	JUL	MAY2019–SEP2019	70	30	
	AUG	JUN2019–OCT2019	60	40	
	SEP	JUL2019–NOV2019	60	40	
	OCT	AUG2019–DEC2019	60	40	

Figure 9 ENSO forecast probabilities based on the El Niño prediction model

Red, yellow and blue bars indicate probabilities that the five-month running mean of the NINO.3 SST deviation from the latest sliding 30-year mean will be +0.5°C or above (El Niño), between +0.4 and -0.4°C (ENSO-neutral) and -0.5°C or below (La Niña), respectively. Regular text indicates past months, and bold text indicates current and future months.

[<< Table of contents](#)

JMA's Seasonal Numerical Ensemble Prediction for Boreal Summer 2019

Based on JMA's seasonal ensemble prediction system, sea surface temperature (SST) anomalies are expected to be above normal in the equatorial Pacific during boreal summer 2019, suggesting El Niño conditions. In association, active convection is expected over the equatorial Pacific, while inactive convection is expected over the Maritime Continent. Focusing on Asia, precipitation amounts are expected to be above normal in and around the equatorial Indian Ocean and the South China Sea and below normal in Indonesia and South Asia.

1. Introduction

This article outlines JMA's dynamical seasonal ensemble prediction for boreal summer 2019 (June – August, referred to as JJA), which was used as a basis for JMA's operational warm-season outlook issued on 24 May 2019. The outlook is based on the seasonal ensemble prediction system of the Coupled Atmosphere-ocean General Circulation Model (CGCM). See the column below for system details.

Section 2 outlines global SST anomaly predictions, and the associated circulation field predictions for the tropics and sub-tropics are described in Section 3. In Section 4, the circulation fields expected for the mid- and high-latitudes of the Northern Hemisphere are discussed.

2. SST anomalies (Figure 10)

Figure 10 shows predicted SSTs (contours) and related anomalies (shading) for JJA. Above-normal anomalies are expected in the central-to-eastern equatorial Pacific, suggesting El Niño conditions. Near- or below-normal SST anomalies are expected in the south-eastern equatorial Indian Ocean and above-normal SST conditions are expected in the western Indian Ocean, potentially suggesting positive IOD-like conditions.

3. Prediction for the tropics and sub-tropics (Figure 11)

Figure 11 (a) shows predicted precipitation (contours) and related anomalies (shading) for JJA. In association with El Niño conditions, above-normal anomalies are expected over the equatorial Pacific and in/around the eastern equatorial Indian Ocean and the South China Sea, while below-normal anomalies are expected in Indonesia and South Asia.

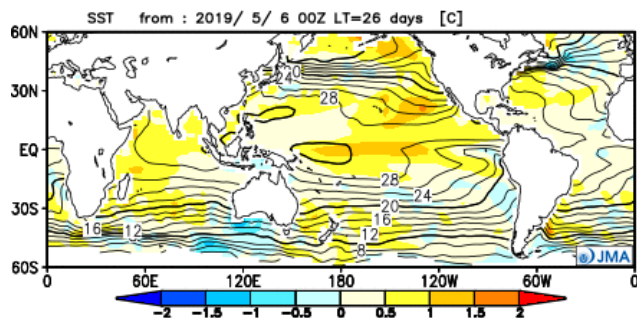


Figure 10 Predicted SSTs (contours) and SST anomalies (shading) for June–August 2019 (ensemble mean of 51 members)

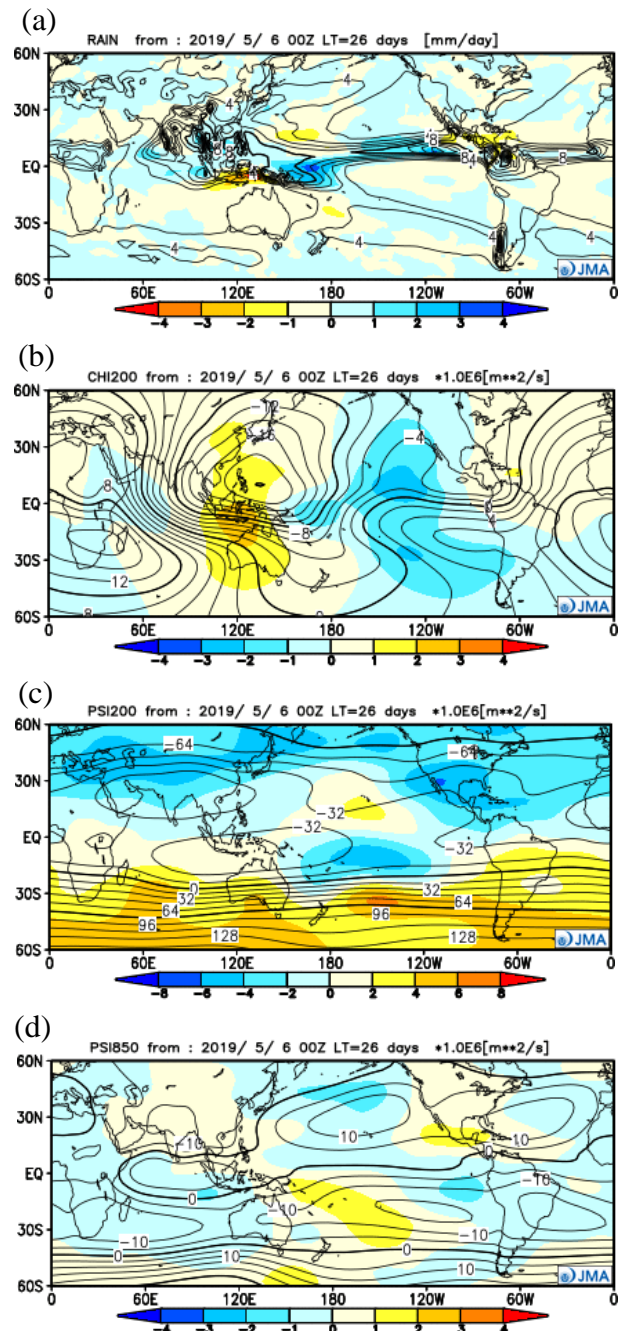


Figure 11 Predicted atmospheric fields from 60°N – 60°S for June–August 2019 (ensemble mean of 51 members)

- (a) Precipitation (contours) and anomaly (shading). The contour interval is 2 mm/day.
- (b) Velocity potential at 200 hPa (contours) and anomaly (shading). The contour interval is 2×10^6 m²/s.
- (c) Stream function at 200 hPa (contours) and anomaly (shading). The contour interval is 16×10^6 m²/s.
- (d) Stream function at 850 hPa (contours) and anomaly (shading). The contour interval is 5×10^6 m²/s.

Figure 11 (b) shows predicted velocity potential (contours) and related anomalies (shading) at the upper troposphere (200 hPa) for JJA. In association with El Niño conditions, negative (i.e., divergent) anomalies are expected over the eastern Pacific, while positive (i.e., convergent) anomalies are expected over the Maritime Continent. Negative (i.e., divergent) anomalies are also expected over the western Indian Ocean, potentially in association with positive IOD-like conditions.

Figure 11 (c) shows predicted stream functions (contours) and related anomalies (shading) at the upper troposphere (200 hPa) for JJA. Negative (i.e., cyclonic) anomalies are expected over Eurasia, indicating a weaker-than-normal Tibetan High and a southward-shifting tendency for the subtropical jet stream. Similar atmospheric circulation patterns have frequently been observed during past El Niño events.

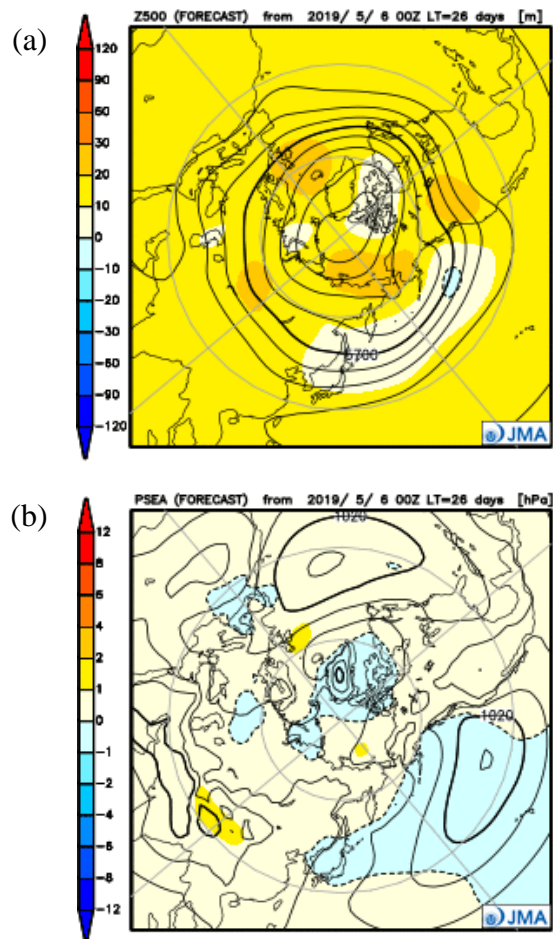
Figure 11 (d) shows predicted stream functions (contours) and related anomalies (shading) at the lower troposphere (850 hPa) for JJA. Equatorial symmetric cyclonic anomalies are expected over the western-to-central Pacific in association with active convection over the Pacific, while equatorial symmetric anti-cyclonic anomalies are predicted in association with inactive convection over the Maritime Continent.

4. Prediction for the mid- and high- latitudes of the Northern Hemisphere

Figure 12 (a) shows predicted geopotential heights (contours) and related anomalies (shading) at 500 hPa for JJA. Positive anomalies are predicted over most of the Northern Hemisphere in association with global warming trends and El Niño conditions. However, relative negative anomalies are expected over the North Pacific in association with positive PNA-like teleconnection, which is a phenomenon frequently observed during past El Niño events.

Figure 12 (b) shows predicted sea level pressure (contours) and related anomalies (shading) for JJA. As with geopotential height, negative anomalies are expected over the North Pacific.

(Takuya Komori, Tokyo Climate Center)



Figures 12 Predicted atmospheric fields from 20°N – 90°N for June–August 2019 (ensemble mean of 51 members)

(a) Geopotential height at 500 hPa (contours) and anomaly (shading). The contour interval is 60 m.

(b) Sea level pressure (contours) and anomaly (shading). The contour interval is 4 hPa.

[<< Table of contents](#)

JMA's Seasonal Ensemble Prediction System

JMA operates a seasonal Ensemble Prediction System (EPS) using the Coupled atmosphere-ocean General Circulation Model (CGCM) to make seasonal predictions beyond a one-month time range. The EPS produces perturbed initial conditions by means of a combination of the initial perturbation method and the lagged average forecasting (LAF) method. The prediction is made using 51 members from the latest four initial dates (13 members are run every 5 days). Details of the prediction system and verification maps based on 30-year hindcast experiments (1981–2010) are available at <http://ds.data.jma.go.jp/tcc/tcc/products/model/>.

Warm Season Outlook for Summer 2019 in Japan

JMA issued warm season outlook for the coming summer (June – August) over Japan in February and updated it on 24 May. This article outlines the update.

1. Outlook summary (Figure 13)

- Seasonal mean temperatures are expected to be near-normal over mainland Japan.
- Seasonal precipitation amounts are expected to exhibit an above-normal tendency over mainland Japan.

2. Outlook background

Figure 14 summarizes expected large-scale oceanic/atmospheric characteristics for the coming summer. The grounds for the outlook are given below.

- El Niño conditions are likely to continue until summer, suggesting that sea surface temperatures (SSTs) will be above normal over the central-to-eastern Pacific.
- Convective activity is expected to be enhanced over the equatorial central Pacific and suppressed over the Asian monsoon region in association with the SST anomaly pattern.
- In the upper troposphere, the subtropical jet stream over Asia is expected to exhibit a southward shift, and the northward extension of the Tibetan High is expected to be weaker than normal due to an inactive Asian monsoon.
- In the lower troposphere, the North Pacific High is expected to be stronger than normal to the south of Japan, while its extension toward Japan is expected to be weaker as a manifestation of the negative Pacific-Japan (PJ) pattern.
- This pattern is expected to bring humid air along the high into the country, and a tendency for wet and rainy mid-summer conditions, rather than hot and sunny weather, is expected.
- Overall temperatures in the troposphere are expected to be above normal due to the prevailing long-term increasing trend. These tendencies are likely to decrease the chance of below-normal temperatures.

(Hiroshi Ohno, Tokyo Climate Center)

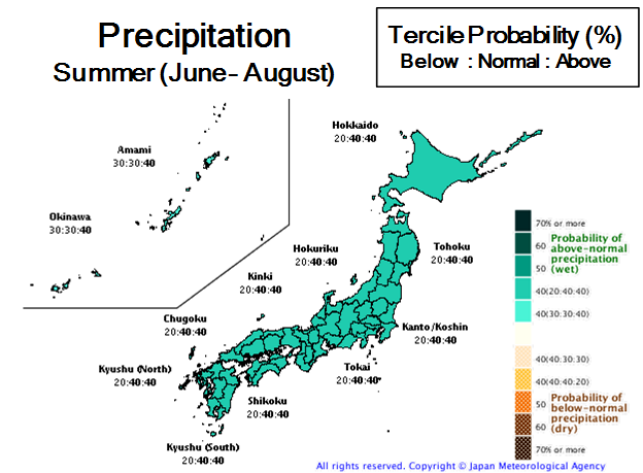
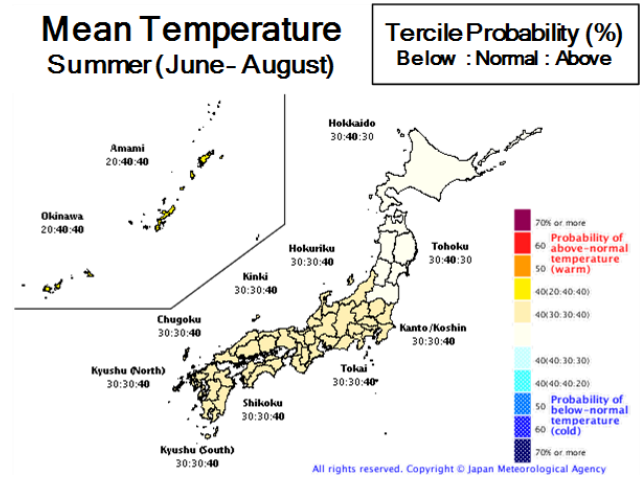


Figure 13 Outlook for summer 2019 temperature (top) and precipitation (bottom) probability in Japan

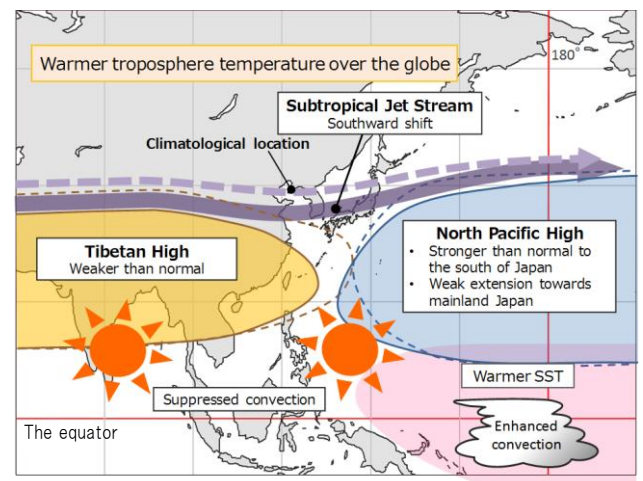


Figure 14 Conceptual diagram showing expected large-scale ocean/atmosphere characteristics for summer 2019

[<< Table of contents](#)

Summary of the 2018/2019 Asian Winter Monsoon

This report summarizes the characteristics of the surface climate and atmospheric/oceanographic considerations related to the Asian winter monsoon for 2018/2019.

Note: The Japanese 55-year Reanalysis (JRA-55; Kobayashi et al., 2015) atmospheric circulation data and COBE-SST (Ishii et al., 2005) sea surface temperature (SST) data were used for this investigation. NOAA Interpolated Outgoing Longwave Radiation (OLR) data (Liebmann and Smith 1996) provided online by the U.S. NOAA Earth System Research Laboratory (ESRL) at <https://www.esrl.noaa.gov/psd/> was referenced to infer tropical convective activity. The base period for the normal is 1981–2010. The term “anomaly” as used in this report refers to deviation from the normal.

1. Surface climate conditions

Temperatures for December 2018 to February 2019 were generally above normal from the eastern part of East Asia to the southern part of South Asia, and were below normal in and around the northwestern part of East Asia (Figure 15). In particular, seasonal mean temperatures were extremely high from the Okinawa/Amami region of Japan to southern China and from the central part of Southeast Asia to the southern part of South Asia, and were extremely low from western Mongolia to northwestern China. Precipitation amounts during this period were above normal in and

around southern and western parts of East Asia and the northwestern part of Southeast Asia, and were below normal in the northeastern part of East Asia (Figure 16). Drier-than-normal conditions in and around the Philippines and warmer-than-normal conditions in and around Southeast Asia, as seen in typical anomaly patterns of past El Niño events, were observed around February.

Figure 17 shows the extreme climate conditions observed between December 2018 and February 2019. In December, extremely high temperatures were seen from the Okinawa region of Japan to Southeast Asia, and extremely low temperatures were seen in the northwestern part of East Asia. Extremely high precipitation amounts were observed from western Japan to eastern China and from Myanmar to northwestern Sumatra. In January, extremely high temperatures were seen from northeastern China to the southern part of Central Siberia and from southern China to the central part of Southeast Asia. Extremely high precipitation amounts were observed from southern China to western Thailand, and extremely low precipitation amounts were observed from northern Japan to the southern Korean Peninsula. In February, extremely high temperatures were seen from the Ogasawara Islands of Japan to southern China and from the central part of Southeast Asia to the southern part of South Asia.

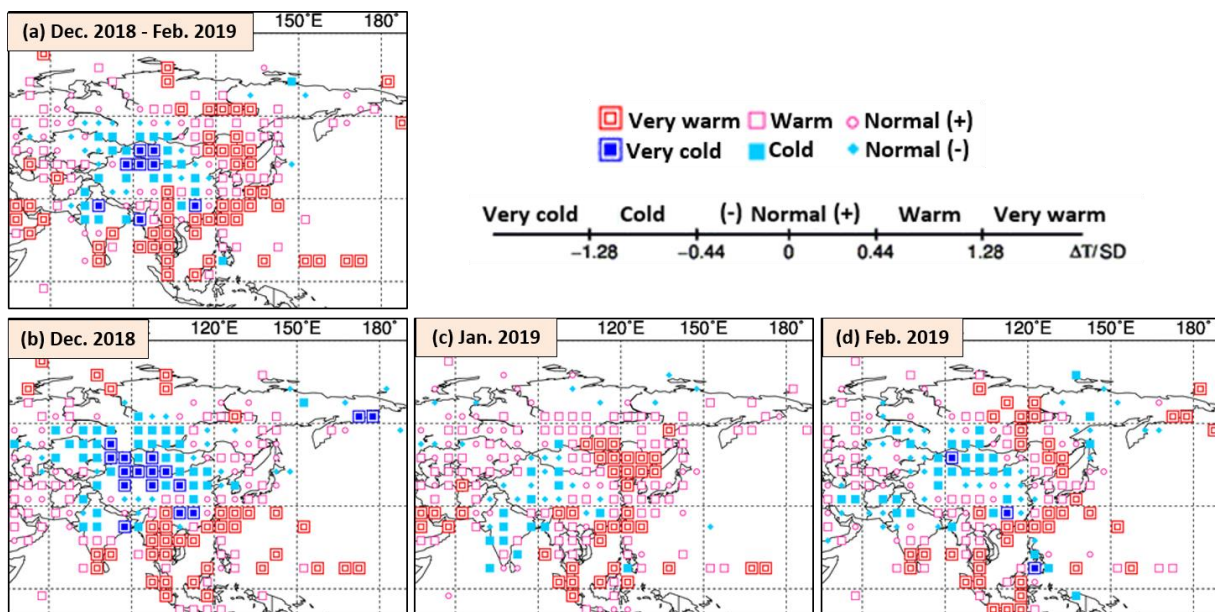


Figure 15 (a) Three-month mean temperature anomalies for December 2018 to February 2019, and monthly mean temperature anomalies for (b) December 2018, (c) January 2019 and (d) February 2019

Categories are defined by the three-month/monthly mean temperature anomaly against the normal divided by its standard deviation and averaged in $5^\circ \times 5^\circ$ grid boxes. The thresholds of each category are -1.28, -0.44, 0, +0.44 and +1.28. Standard deviations were calculated from 1981–2010 statistics. Areas over land without graphical marks are those where observation data are insufficient or where normal data are unavailable.

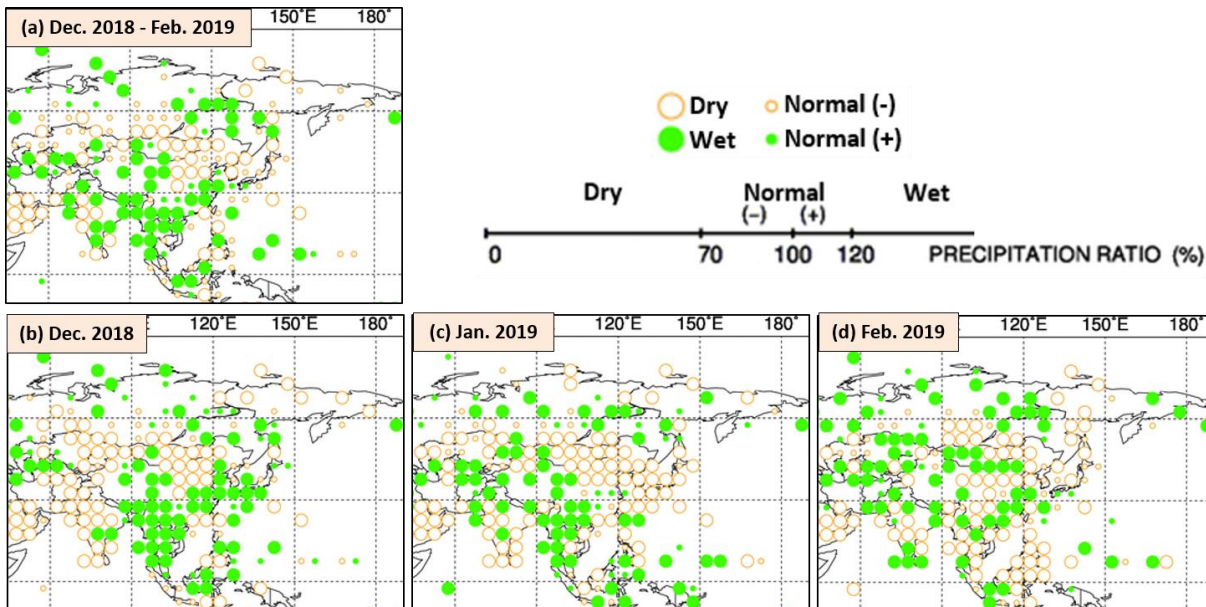


Figure 16 Three-month total precipitation ratio for December 2018 to February 2019, and monthly total precipitation ratio for (b) December 2018, (c) January 2019 and (d) February 2019

Categories are defined by the three-month mean precipitation ratio against the normal and averaged in $5^\circ \times 5^\circ$ grid boxes. The thresholds of each category are 70, 100 and 120%. Areas over land without graphical marks are those where observation data are insufficient or where normal data are unavailable.

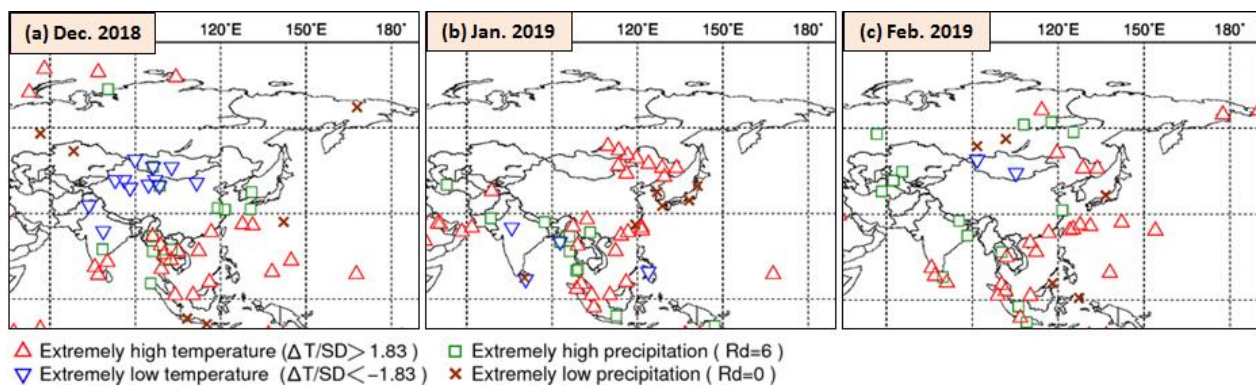


Figure 17 Extreme climate stations for (a) December 2018, (b) January 2019 and (c) February 2019

ΔT , SD and Rd indicate temperature anomaly, standard deviation and quintile, respectively.

2. Characteristic atmospheric circulation and oceanographic conditions

2.1 Conditions in the tropics

The El Niño conditions that developed in boreal autumn 2018 continued during winter 2018/2019. Positive SST anomalies were observed over almost the whole of the equatorial Pacific and in the equatorial Indian Ocean. In the North Pacific, remarkably positive SST anomalies were observed from the South China Sea to the central part (Figure 18).

Convective activity inferred from OLR during this period was enhanced to the west of the date line and suppressed from the southeastern tropical Indian Ocean to the Maritime Continent and around the Philippines (Figure 19). Over the Indochina Peninsula and the Malay Peninsula, where precipitation amounts during this period were above normal (Figure 16 (a)), convective activity was enhanced in December and January.

In the upper troposphere, large-scale divergent anomalies were seen over areas near the date line in association with enhanced convective activity, and convergent anomalies were observed over the Maritime Continent (Figure 20 (a)). In the 200-hPa stream function field, cyclonic circulation anomalies straddling the equator were seen over the Maritime Continent. A wave train was seen along the subtropical jet stream, with cyclonic circulation anomalies over northern India and anti-cyclonic circulation anomalies over the Middle East and the East China Sea (Figure 20 (b)). In the lower troposphere, cyclonic circulation anomalies straddling the equator were seen from west of the date line to the central Pacific, and anti-cyclonic circulation anomalies were seen around the Philippines (Figure 20 (c)).

The active phase of equatorial intraseasonal oscillation propagated eastward globally during winter 2018/2019 except in early February (Figure 21).

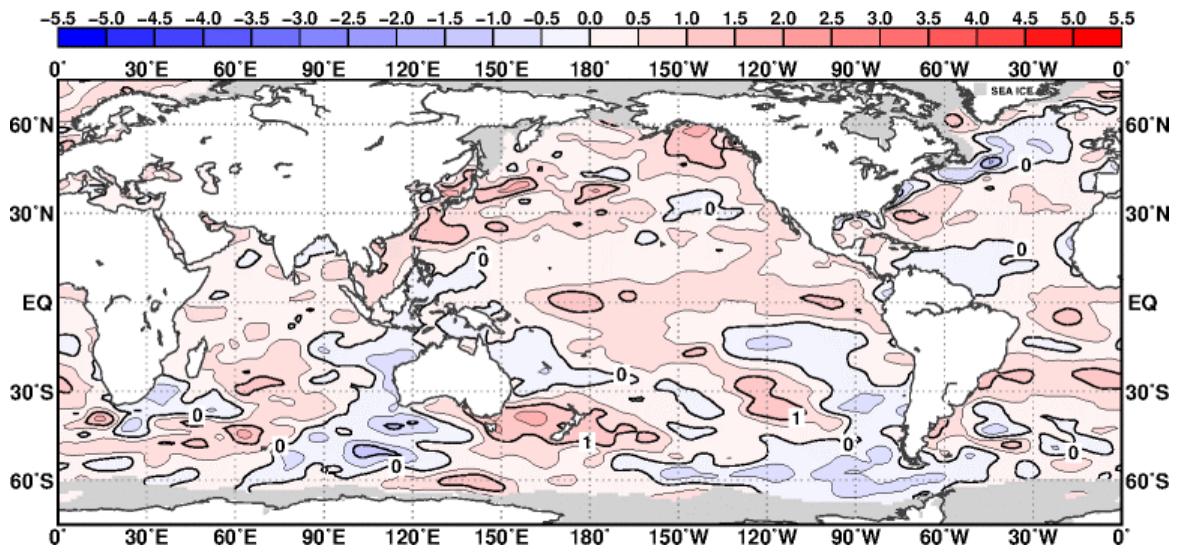


Figure 18 Three-month mean sea surface temperature (SST) anomalies [$^{\circ}\text{C}$] for December 2018 to February 2019

The contour interval is 0.5°C .

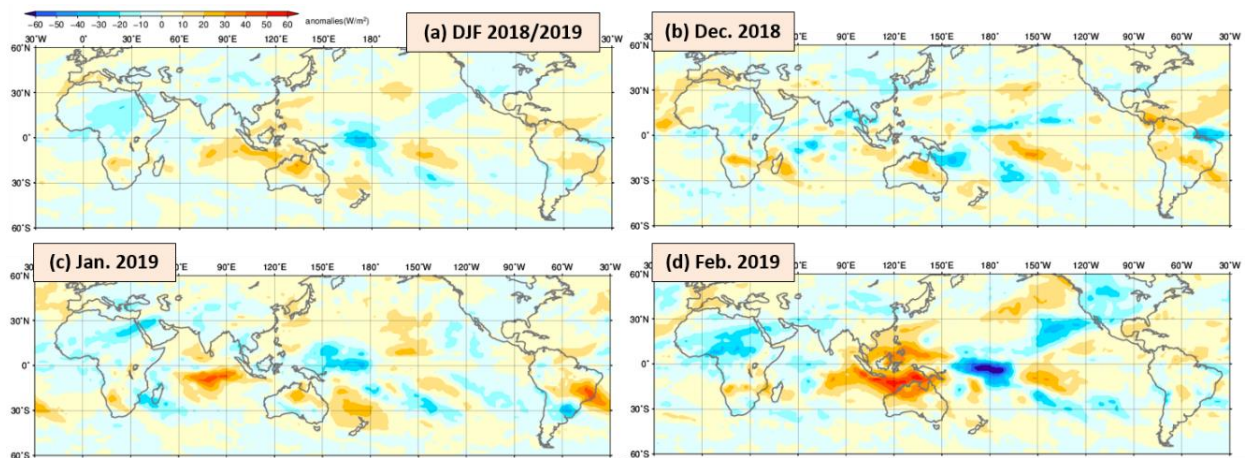


Figure 19 Outgoing longwave radiation (OLR) anomalies [W/m^2] (a) averaged over the three months from December 2018 to February 2019, for (b) December 2018, (c) January 2019 and (d) February 2019

The blue and red shading indicates areas of enhanced and suppressed convective activity, respectively.

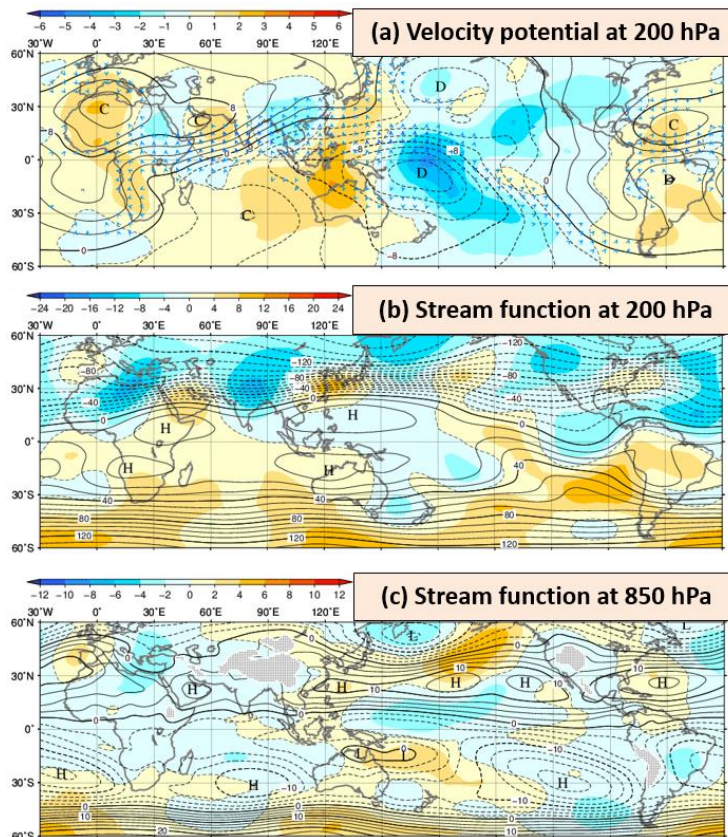


Figure 20 Three-month mean (a) 200-hPa velocity potential, (b) 200-hPa stream function, and (c) 850-hPa stream function for December 2018 to February 2019 [unit: $10^6 \text{ m}^2/\text{s}$]

(a) The contours indicate velocity potential at intervals of $2 \times 10^6 \text{ m}^2/\text{s}$, and the shading shows velocity potential anomalies. D and C indicate the bottom and the peak of velocity potential, corresponding to the centers of large-scale divergence and convergence, respectively (b, c). The contours indicate stream function at intervals of (b) 10 and (c) $2.5 \times 10^6 \text{ m}^2/\text{s}$, and the shading shows stream function anomalies. H and L denote the centers of anticyclonic and cyclonic circulations, respectively.

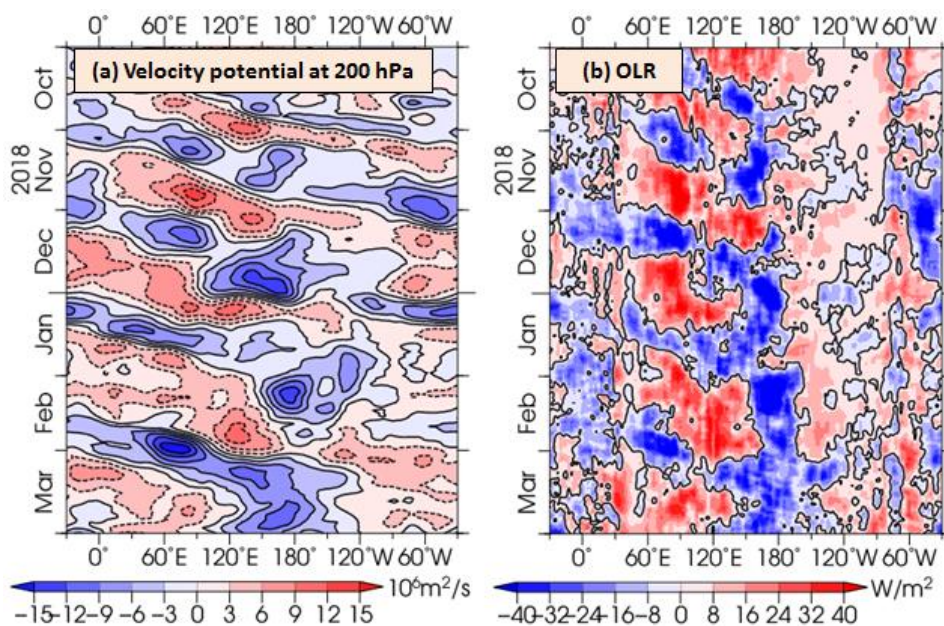


Figure 21 Time-longitude cross section of seven-day running mean (a) 200-hPa velocity potential anomalies [$10^6 \text{ m}^2/\text{s}$] and (b) outgoing longwave radiation (OLR) anomalies [W/m^2] around the equator ($5^\circ\text{S} - 5^\circ\text{N}$) for October 2018 to March 2019

(a) The blue and red shading indicates areas of divergence and convergence anomalies, respectively. (b) The blue and red shading indicates areas of enhanced and suppressed convective activity, respectively.

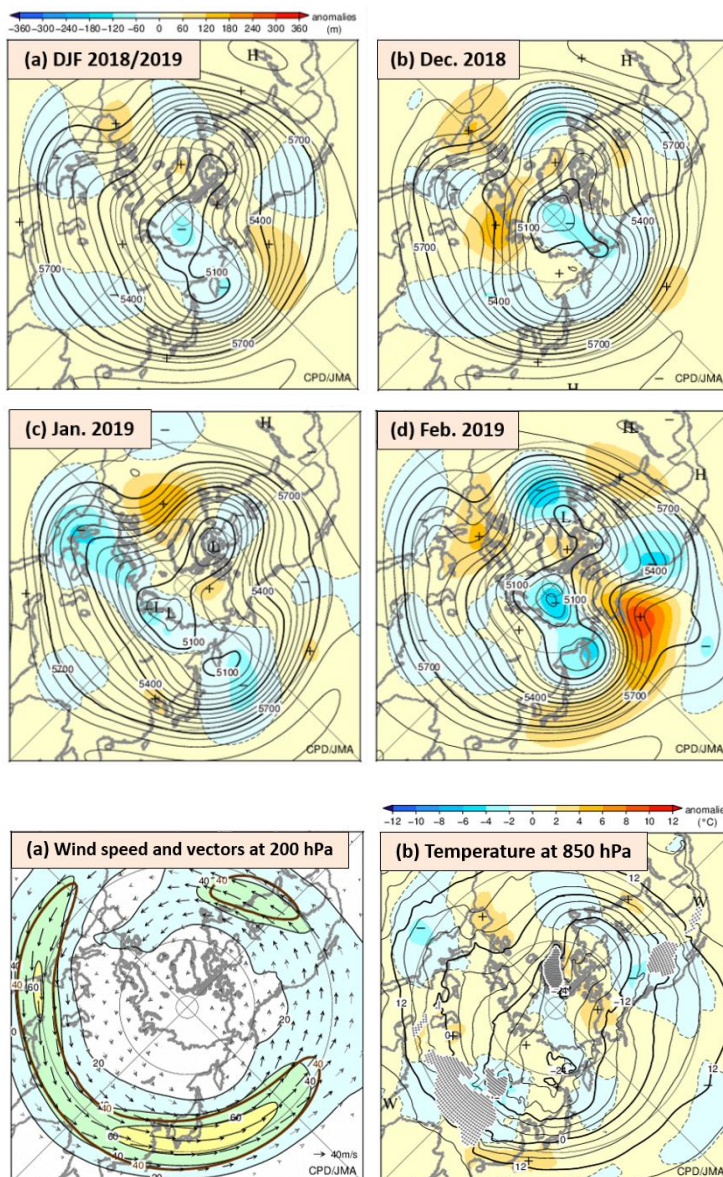
2.2 Conditions in the extratropics

In the 500-hPa height field during winter 2018/2019, the polar vortex was centered near the North Pole and over the Kamchatka Peninsula. A wave train was seen over mid-latitudes with positive anomalies from eastern China to the seas east of Japan, and negative anomalies were seen from the western part of East Asia to the northern part of South Asia (Figure 22 (a)). Zonally elongated positive anomalies were seen from Japan to the area east of the country in December and February (Figure 22 (b), (d)).

The subtropical jet stream from North Africa to Eurasia meandered. The westerly jet stream shifted northward of its normal position from eastern China to Japan (Figure 23 (a)). Temperatures at 850 hPa (Figure 23 (b)) were above normal from southern China to the seas south of Japan, and were below normal over the northwestern part of East Asia.

In the sea level pressure field (Figure 24), negative anomalies were seen near the Kamchatka Peninsula throughout the period, indicating a northwestward shift of Aleutian Low activity. The Siberian High was stronger than normal over its normal position, and its eastward extension was weaker than normal. Positive anomalies were seen from Japan to the area east of the country in December and February.

(Hitoshi Sato, Tokyo Climate Center)



References

- Ishii, M., A. Shouji, S. Sugimoto and T. Matsumoto, 2005: Objective Analyses of Sea-Surface Temperature and Marine Meteorological Variables for the 20th Century using ICOADS and the Kobe Collection. *Int. J. Climatol.*, **25**, 865-879.
- Kobayashi, S., Y. Ota, Y. Harada, A. Ebata, M. Moriya, H. Onoda, K. Onogi, H. Kamahori, C. Kobayashi, H. Endo, K. Miyaoka, and K. Takahashi, 2015: The JRA-55 Reanalysis: General Specifications and Basic Characteristics. *J. Meteorol. Soc. Japan*, **93**, 5 – 48.
- Liebmann, B., and C. A. Smith, 1996: Description of a complete (interpolated) outgoing longwave radiation dataset. *Bull. Amer. Meteor. Soc.*, **77**, 1275–1277.

Figure 22 500-hPa height [m] (a) averaged over the three months from December 2018 to February 2019, for (b) December 2018, (c) January 2019 and (d) February 2019

The contours indicate 500-hPa height at intervals of 60 m, and the shading denotes anomalies. H and L indicate the peak and bottom of 500-hPa height, respectively, and + (plus) and – (minus) show the peak and bottom of anomalies, respectively.

Figure 23 Three-month mean (a) 200-hPa wind speed and vectors [m/s] and (b) 850-hPa temperature [°C] for December 2018 to February 2019

(a) The black lines show wind speed at intervals of 20 m/s, and the brown lines show its normal at intervals of 40 m/s. (b) The contours indicate 850-hPa temperature at intervals of 4 °C and the shading shows related anomalies.

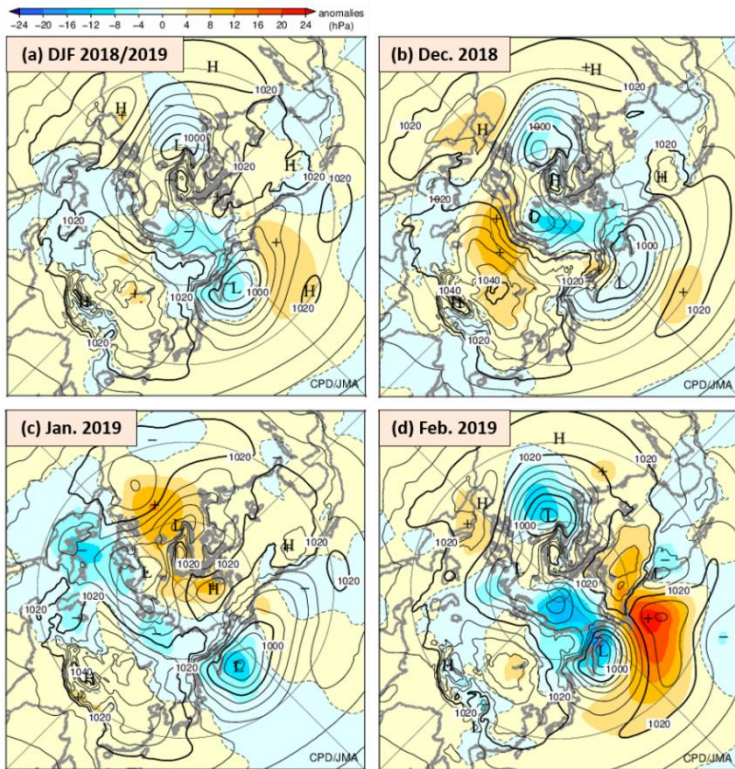


Figure 24 Sea level pressure [hPa] (a) averaged over the three months from December 2018 to February 2019, for (b) December 2018, (c) January 2019 and (d) February 2019
 The contours indicate sea level pressure at intervals of 4 hPa, and the shading shows related anomalies. H and L indicate the centers of high and low pressure systems, respectively, and + (plus) and – (minus) show the peak and bottom of sea level pressure anomalies, respectively.

[<< Table of contents](#)

TCC contributions to Regional Climate Outlook Forums in Asia

WMO Regional Climate Outlook Forums (RCOFs) bring together national, regional and international climate experts on an operational basis to produce regional climate outlooks based on input from participating NMHSs, regional institutions, Regional Climate Centers and global producers of climate predictions. By providing a platform for countries with similar climatological characteristics to discuss related matters, these forums ensure consistency in terms of access to and interpretation of climate information. In spring 2019, TCC experts participated in two RCOFs in Asia.

1. FOCRA II

The first RCOF was held at the 15th session of the Forum on Regional Climate Monitoring, Assessment and Prediction for Regional Association II (FOCRA II) in Nanning, China, from 8 to 10 May. At the event, experts from about 20 countries/territories made presentations in six sessions featuring talks by invited lecturers and other oral presentations. TCC attendees gave two presentations outlining the characteristics of the last winter monsoon and the outlook for this summer based on JMA's seasonal Ensemble Prediction System (EPS). The presentations contributed to discussions on a consensus outlook for the coming summer.

2. SASCOF

The Government of Nepal's Department of Hydrology and Meteorology (DHM) hosted the 14th summer session of the South Asian Climate Outlook Forum (SASCOF-14) and the Pre-COF Training Workshop from 18 to 23 April 2019 in Kathmandu, Nepal.

The forum was supported by the World Meteorological Organization (WMO), the Regional Climate Center (RCC) Pune of India Meteorological Department (IMD), UK Met Office (UKMO), and the Regional Integrated Multi-hazard Early-warning System for Africa and Asia (RIMES) with funding from the Asia – Regional Resilience to Changing Climate (ARRCC) program based on UKMO and RIMES collaboration. Attendees discussed the climatic conditions of the upcoming summer monsoon season, which lasts from June to September.

As part of the activities of WMO's World Meteorological Centre (WMC), an expert from WMC Tokyo provided a summer monsoon season outlook based on JMA's dynamical seasonal ensemble prediction system, with probabilistic information on atmospheric variability and the evolution of conditions in the tropical Pacific and Indian Ocean areas. The provision of this information was intended to support the output of country-scale outlooks by National Meteorological and Hydrological Services (NMHSs) in South Asia and contribute to the summarizing a consensus outlook for South Asia.

The forum placed particular emphasis on the Climate Services User Forum (CSUF) with focus on the water and agriculture sectors based on the sharing of information with user sectors to support discussion of their experiences of using climatic services. The WMC Tokyo expert was also involved in the active discussion to promote better use of climate services through future SASCOF activities.

(FOCRA II: Akira Ito and Masashi Sumitomo, SASCOF-14: Takuya Komori, Tokyo Climate Center)



Akira Ito presenting seasonal forecast for this summer (left) and Masashi Sumitomo presenting characteristics of the last winter monsoon (right) at FOCRA II.

[<< Table of contents](#)

JMA Advisory Panel on Extreme Climate Events: collaboration between research and operation in Japan to provide useful climate services

[The Future of Climate Services \(Allis et al., 2019\)](#) in [WMO Bulletin Vol. 68 \(1\) – 2019](#) provides overviews of various current activities and future challenges regarding climate services in the WMO community. It includes a section featuring the Japan Meteorological Agency (JMA) Advisory Panel on Extreme Climate Events (referred to here simply as “the Panel”) to enhance collaboration between the areas of research and operation toward the provision of useful climate services in Japan. The Panel is described in more detail here, with updates from TCC News [No. 9](#) and [No. 28](#).

There is a widely recognized need to develop and sustain links between the research community and operational service providers such as NMHSs (National Meteorological and Hydrological Services) in order to expedite the application of research advances in operational climate services for improved climate information. The Panel, established in 2007, consists of prominent climate scientists from universities and research institutes in Japan, and has been chaired by Professor Hisashi Nakamura of the University of Tokyo since 2017. Its missions are: a) to investigate factors behind extreme climate events in Japan; b) to advise and assist JMA on the issuance of statements on such events; and c) to recommend related application of state-of-the-art findings and expertise. A working group under the Panel assists with the production of materials and research relating to Panel discussions.

When a nationwide-scale extreme climate event significantly impacts socio-economic activity in Japan, the Panel initiates investigation and discussion on factors of the events with JMA experts. In this context, a preliminary e-mail discussion is followed by more detailed face-to-face discussions. Shortly after the meeting, JMA issues a statement outlining factors and outlooks relating to the event based on the Panel’s investigation and advice. In 2018 summer, Japan experienced unprecedented heavy rainfall, namely “The Heavy Rain Event of July 2018”, followed by extremely high temperatures ([TCC, 2018: Primary Factors behind the Heavy Rain Event of July 2018 and the Subsequent Heatwave in Japan from Mid-July Onward](#)). The statement is provided to decision makers and the general public in Japan to help prevent or minimize adverse effects

from extreme events. In addition, the results of discussions were summarized in a peer-reviewed paper (Shimpo et al., 2019) produced with close collaboration between JMA experts and the Panel.

To support the effectiveness and efficiency of the Panel’s investigations, JMA regularly shares various forms of data, products and tools to help clarify current conditions of the climate system via a dedicated website for the Panel and to support online/email discussions on climate diagnostics with Panel members. JMA provides the Panel both with its own products and with others created using programs provided by Panel members themselves, thereby helping to improve analysis of factors behind extreme events.

This framework provides high value by enabling JMA to improve its operational climate information and services (including those provided to NMHSs in Regional Association (RA) II by the Tokyo Climate Center in its role as a WMO RA II Regional Climate Centre) as well as staff expertise based on the progressive and state-of-the-art research findings of the Panel. Based on this arrangement, Panel members can make significant contributions to society using their advanced expertise in the area of climate science. The regular updating of online climate data and products helps Panel members to comprehend the characteristics of ongoing phenomena and provides materials for the identification of related research seeds. It should be emphasized that collaboration between research and operational services (as in the activities reported here) must lead to a win-win situation in order to enhance the sustainability of engagement.

(Akihiko Shimpo, Tokyo Climate Center)

Reference

Allis et al., 2019: The Future of Climate Services. [WMO Bulletin Vol. 68 \(1\)](#), 50-58

Shimpo, A. et al., 2019: Primary Factors behind the Heavy Rain Event of July 2018 and the Subsequent Heat Wave in Japan. *SOLA*, **15A**, in press, doi:10.2151/sola.15A-003.

[<< Table of contents](#)

You can also find the latest newsletter from Japan International Cooperation Agency (JICA).

JICA’s World (April 2019)

<https://www.jica.go.jp/english/publications/j-world/c8h0vm0000epfpe0-att/1904.pdf>

JICA’s World is the quarterly magazine published by JICA. It introduces various cooperation projects and partners along with the featured theme. The latest issue features “Infectious Disease Control Japanese Technology Saving Lives”.

Any comments or inquiry on this newsletter and/or the TCC website would be much appreciated. Please e-mail to tcc@met.kishou.go.jp.

(Editors: Yasushi Takatsuki, Yasushi Mochizuki and Kazuaki Tsuji)

Tokyo Climate Center (TCC), Japan Meteorological Agency
Address: 1-3-4 Otemachi, Chiyoda-ku, Tokyo 100-8122, Japan
TCC Website: <http://ds.data.jma.go.jp/tcc/tcc/index.html>